



Apalowo, R.K. and Chronopoulos, D. and Thierry, V.
(2017) Thermal effect on wave interaction in composite structures. In: : 19th International Conference on Aerospace, Mechanical, Automotive and Materials Engineering, 19-20 January 2017, London, UK.

Access from the University of Nottingham repository:

<http://eprints.nottingham.ac.uk/52468/1/Conf2.pdf>

Copyright and reuse:

The Nottingham ePrints service makes this work by researchers of the University of Nottingham available open access under the following conditions.

This article is made available under the University of Nottingham End User licence and may be reused according to the conditions of the licence. For more details see:
http://eprints.nottingham.ac.uk/end_user_agreement.pdf

A note on versions:

The version presented here may differ from the published version or from the version of record. If you wish to cite this item you are advised to consult the publisher's version. Please see the repository url above for details on accessing the published version and note that access may require a subscription.

For more information, please contact eprints@nottingham.ac.uk

Thermal Effect on Wave Interaction in Composite Structures

R.K. Apalowo, D. Chronopoulos and V. Thierry

Abstract—There exist a wide range of failure modes in composite structures due to the increased usage of the structures especially in aerospace industry. Moreover, temperature dependent wave response of composite and layered structures have been continuously studied, though still limited, in the last decade mainly due to the broad operating temperature range of aerospace structures. A wave finite element (WFE) and finite element (FE) based computational method is presented by which the temperature dependent wave dispersion characteristics and interaction phenomenon in composite structures can be predicted. Initially, the temperature dependent mechanical properties of the panel in the range of -100°C to 150°C are measured experimentally using the Thermal Mechanical Analysis (TMA). Temperature dependent wave dispersion characteristics of each waveguide of the structural system, which is discretized as a system of a number of waveguides coupled by a coupling element, is calculated using the WFE approach. The wave scattering properties, as a function of temperature, is determined by coupling the WFE wave characteristics models of the waveguides with the full FE modelling of the coupling element on which defect is included. Numerical case studies are exhibited for two waveguides coupled through a coupling element.

Index Terms—Temperature dependent mechanical characteristics, Wave propagation properties, Damage detection, Wave finite element, Composite structure.

I. INTRODUCTION

Composite structures are being increasingly used in many industrial fields, such as aerospace and military, due to their versatile physical and mechanical properties. However, an aerospace structure typically operates within a broad temperature range, varying between 100°C to 200°C for launch vehicles and 60°C to $+50^{\circ}\text{C}$ for aircrafts. Hence, an attempt is made in order to exhibit the sensitivity of the wave interaction properties of a composite structure to the ambient flight temperature.

Recently, the effect of high temperature on the thermomechanical response of various composite structures, such as multi-layered plates and shells [1], glass epoxy composites [2], [3] and carbon fibre epoxy composites [4], [5], has been extensively assessed. However, investigation of the thermoacoustic behaviour of composites has been found almost inexistent in the open literature. So, there is a great need for the investigation of temperature dependent dynamic behaviour of composite laminates. Of particular importance is investigating the interaction of wave propagation with damage with respect to temperature.

Wave propagation damage detection methods are based on calculating the reflection and transmission coefficients at the point of inhomogeneity. Of these, the Wave and Finite Element (WFE) method [6], [7], [8], [9] is one of the most efficient

computational methods suitable for predicting the vibrational response and wave interaction with damage in various types of structures. The method has recently found applications in predicting the vibroacoustic and dynamic performance of composite panels and shells [10], [11], [12], [13], [14], [15], [16], with pressurized shells [17], [18] and complex periodic structures [19], [20], [21] having been investigated. The variability of acoustic transmission through layered structures [22], [23], as well as wave steering effects in anisotropic composites [24] have been modelled through the same methodology. However, this numerical method has not been implemented to investigate the effect of temperature on wave scattering. Temperature dependent wave interaction properties would be useful for structural defect and evaluation within broad range of temperature.

In this work, the effect of temperature on the wave interaction of composite laminates is considered. The temperature dependent mechanical properties of the laminate constituents materials are experimentally calculated using the Thermal Mechanical Analysis. A WFE approach is used to calculate the wave propagation properties, and then coupled to finite element modelling of the coupling joint in order to calculate wave interaction coefficients from the joint. The paper is organised as follows. Section II presents the experimental measurement of the temperature dependent mechanical properties of the composite facesheet and core materials. Section III presents the calculations waves propagation properties. Waves interaction modelling is presented in Section IV. Numerical examples are presented in Section V. Section VI presents concluding remarks of the work.

II. MEASUREMENT OF MECHANICAL CHARACTERISTICS

A Thermal Mechanical Analysis (TMA) device is used to measure the mechanical characteristics of a sandwich panel comprising of a carbon epoxy facesheet and a quasi-isotropic honeycomb core, which absorbs and adheres to the resin in which the facesheet is impregnated. In the polymerisation process, the resin serves as the facesheet matrix as well as the binding agent. The nominal mechanical characteristics of the composite panel's constituents at 20°C are shown in Table I. Measurements are made at a temperature range of -5°C to 150°C .

Respective segments of the facesheet and the core materials are subjected to longitudinal traction (Fig. 1) and shear deformation (Fig. 2) respectively in order to determine the elastic and shear moduli respectively

TABLE I
NOMINAL MECHANICAL PROPERTIES OF THE COMPOSITE LAMINATE'S
CONSTITUENTS AT 20°C

Carbon Epoxy	Honeycomb foam
$E = 54 \text{ GPa}$	$E_x = 85 \text{ MPa}$
$\rho = 1410 \text{ kg/m}^3$	$E_y = 85 \text{ MPa}$
$\nu = 0.09$	$\rho = 48 \text{ kg/m}^3$
	$\nu_{xy} = 0.23$
	$G_{yz} = 44 \text{ MPa}$
	$G_{xz} = 44 \text{ MPa}$



Fig. 1. Configuration of a segment of the facesheet traction test in the TMA device



Fig. 2. Configuration of a segment of the core shear deformation in the TMA device

The measured elastic (Fig. 3) and shear (Fig. 2) moduli decrease slightly while their corresponding material loss ratios increase slightly with respect to temperature until 110°C, where the glass transition occurs. Beyond this temperature, the moduli and the loss factor decrease rapidly, then the loss factor (about 130°C) start increasing again due to the high viscosity of the resin.

III. WAVE PROPAGATION BY A WAVE AND FINITE ELEMENT METHOD

Wave propagation along the x direction of an arbitrary layered structural waveguide (Fig. 5) is modelled by a WFE method using the transfer matrix approach [25].

By the WFE method, a periodic segment (of length equivalent to one element along x) is modelled. The frequency and temperature dependent dynamic stiffness matrix (DSM) of the segment is given as

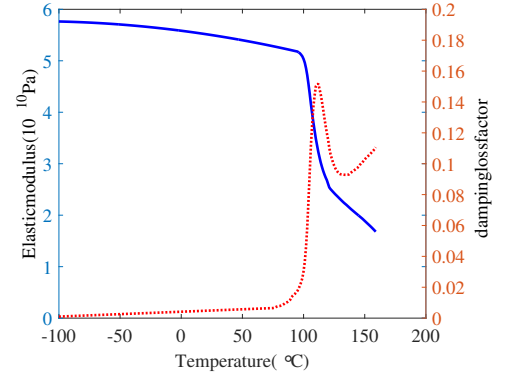


Fig. 3. Experimentally measured temperature dependent elastic modulus (-) and material loss factor (···) for the facesheet material

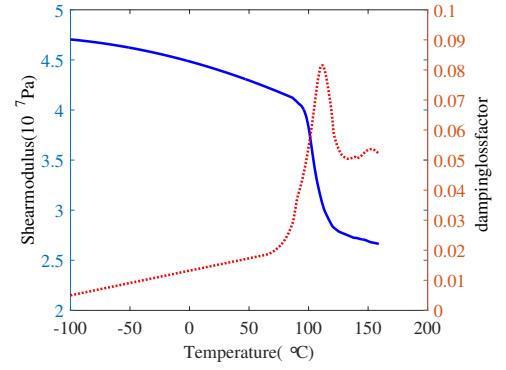


Fig. 4. Experimentally measured temperature dependent shear modulus (-) and material loss factor (···) for the honeycomb core material

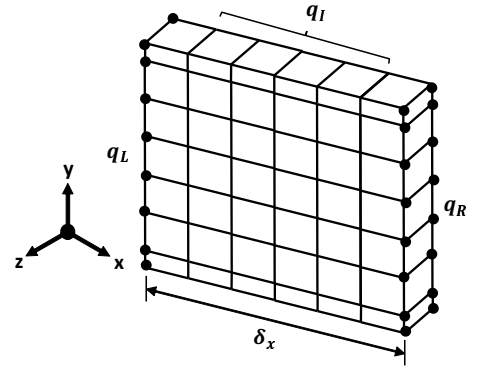


Fig. 5. WFE modelled waveguide with left and right side nodes bullet marked. Range of interior nodes also illustrated

$$\mathbf{D}(\omega, T) = \mathbf{K}(\omega, T) - \omega^2 \mathbf{M}(\omega) + i\omega \mathbf{C}(\omega, T) \quad (1)$$

where \mathbf{K} , \mathbf{M} and \mathbf{C} are the temperature dependent stiffness, mass and damping matrices of the FE model for each considered frequency and temperature. The DSM can be partitioned with respect to left, right and internal DoFs as

$$\begin{bmatrix} \mathbf{D}_{LL} & \mathbf{D}_{LI} & \mathbf{D}_{LR} \\ \mathbf{D}_{IL} & \mathbf{D}_{II} & \mathbf{D}_{IR} \\ \mathbf{D}_{RL} & \mathbf{D}_{RI} & \mathbf{D}_{RR} \end{bmatrix} \begin{Bmatrix} \mathbf{q}_L \\ \mathbf{q}_I \\ \mathbf{q}_R \end{Bmatrix} = \begin{Bmatrix} \mathbf{f}_L \\ \mathbf{0} \\ \mathbf{f}_R \end{Bmatrix} \quad (2)$$

with \mathbf{q} and \mathbf{f} the displacement and forcing vectors respectively. Using a Guyan-type condensation for the internal DoFs, the problem can be expressed as

$$\begin{bmatrix} \mathbf{D}_{LL}^* & \mathbf{D}_{LR}^* \\ \mathbf{D}_{RL}^* & \mathbf{D}_{RR}^* \end{bmatrix} \begin{Bmatrix} \mathbf{q}_L \\ \mathbf{q}_R \end{Bmatrix} = \begin{Bmatrix} \mathbf{f}_L \\ \mathbf{f}_R \end{Bmatrix} \quad (3)$$

Assuming no external forces are applied, the displacement continuity and force equilibrium at the interface of two consecutive periodic segments r and $r+1$ are given as

$$\mathbf{q}_R^{(r)} = \mathbf{q}_L^{(r+1)}; \quad \mathbf{f}_R^{(r)} = -\mathbf{f}_L^{(r+1)} \quad (4)$$

combining Eqs. (3) and (4) gives

$$\begin{Bmatrix} \mathbf{q}_L^{(r+1)} \\ \mathbf{f}_L^{(r+1)} \end{Bmatrix} = \mathbf{T} \begin{Bmatrix} \mathbf{q}_L^{(r)} \\ \mathbf{f}_L^{(r)} \end{Bmatrix} \quad (5)$$

where matrix \mathbf{T} is the symplectic transfer matrix expressed as

$$\mathbf{T} = \begin{bmatrix} -\mathbf{D}_{LR}^{*-1} \mathbf{D}_{LL}^* & \mathbf{D}_{LR}^{*-1} \\ -\mathbf{D}_{RL}^* + \mathbf{D}_{RR}^* \mathbf{D}_{LR}^{*-1} \mathbf{D}_{LL}^* & -\mathbf{D}_{RR}^* \mathbf{D}_{LR}^{*-1} \end{bmatrix} \quad (6)$$

The propagation constant $\lambda = \exp^{-ik\delta_x}$ of the wave relates the right and left nodal displacements and forces as

$$\lambda \mathbf{q}_L^{(r)} = \mathbf{q}_R^{(r)}; \quad -\lambda \mathbf{f}_L^{(r)} = \mathbf{f}_R^{(r)} \quad (7)$$

and substituting Eqs. (4) and (7) into Eq. (5) gives the eigenproblem

whose eigenvalues and eigenvectors solution sets provide a comprehensive description of propagation constants and wave modes of waves along the waveguide at specified frequency and temperature.

IV. WAVE INTERACTION BY A HYBRID WFE/FE METHOD

Consider two waveguides connected through a coupling joint (Fig. 5). The joint is fully FE modelled and can contain damage, geometric or material inconsistencies.

The wavemodes, obtained at each frequency and temperature, for each waveguide in the system can be grouped as

$$\Phi = \begin{bmatrix} \Phi_q^{inc} & \Phi_q^{ref} \\ \Phi_f^{inc} & \Phi_f^{ref} \end{bmatrix} \quad (8)$$

where *inc* and *ref* denote the positive and negative going waves respectively. The modes of the two waveguides in the system can be grouped as

$$\Psi_q^{inc} = \begin{bmatrix} \Phi_{q1}^{inc} & \mathbf{0} \\ \mathbf{0} & \Phi_{q2}^{inc} \end{bmatrix} \quad (9)$$

with similar expressions for Ψ_q^{ref} , Ψ_f^{inc} and Ψ_f^{ref} . Assuming modal decomposition, the physical domain can be converted to the wave domain as

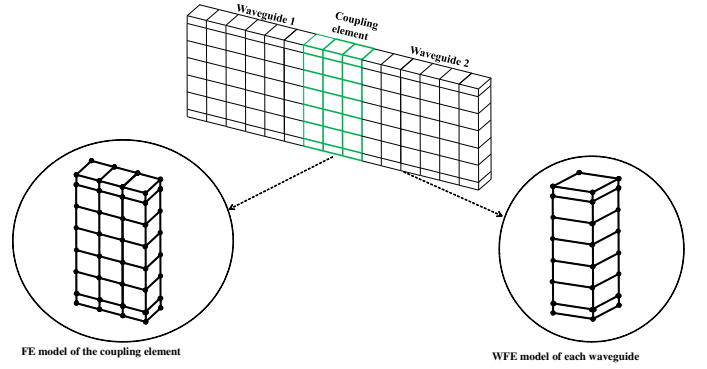


Fig. 6. Caption of a system as two collinear waveguides connected through a coupling joint

$$\begin{Bmatrix} \mathbf{q}_L \\ \mathbf{f}_L \end{Bmatrix} = \Phi \begin{Bmatrix} \mathbf{Q}^{inc} \\ \mathbf{Q}^{ref} \end{Bmatrix} \quad (10)$$

where \mathbf{Q} denotes the amplitudes of the wave modes.

The DSM of the joint can be partitioned with regard to the interface and non-interface nodes with the waveguides as

$$\begin{bmatrix} \mathbf{D}_{11} & \mathbf{D}_{12} \\ \mathbf{D}_{21} & \mathbf{D}_{22} \end{bmatrix} \begin{Bmatrix} \mathbf{q}_1 \\ \mathbf{q}_2 \end{Bmatrix} = \begin{Bmatrix} \mathbf{f}_1 \\ \mathbf{f}_2 \end{Bmatrix} \quad (11)$$

where subscript 1 corresponds to the interface DoFs and 2 the non-interface DoFs. Condensing the non-interface DoFs, the DSM can be expressed as

$$\mathbf{D}_C^* = \mathbf{D}_{11} - \mathbf{D}_{12} \mathbf{D}_{22}^{-1} \mathbf{D}_{21} \quad (12)$$

Applying displacement continuity and equilibrium of forces at the connecting interfaces, the scattering matrix \mathbf{S} of the joint, whose partitions relate the amplitudes of the incident and scattered waves as

$$\begin{Bmatrix} \mathbf{Q}_1^{ref} \\ \mathbf{Q}_2^{ref} \end{Bmatrix} = \mathbf{S} \begin{Bmatrix} \mathbf{Q}_1^{inc} \\ \mathbf{Q}_2^{inc} \end{Bmatrix} \quad (13)$$

where

$$\mathbf{S} = -[\Psi_f^{ref} - \mathbf{D}_C^* \Psi_q^{ref}]^{-1} [\Psi_f^{inc} - \mathbf{D}_C^* \Psi_q^{inc}] \quad (14)$$

with diagonal elements being the reflection coefficients and off the diagonal the transmission coefficients of the scattered waves.

V. NUMERICAL RESULTS

The methodology presented in this work is demonstrated on two numerical case examples: two collinear rods connected through a finite joint, and two sandwich laminates connected through a laminate joint. Calculations are made at five different temperatures, -100, 25, 90, 110 and 150°C for the composite laminate example and at three different temperatures, 25, 90 and 150°C for the rod example.

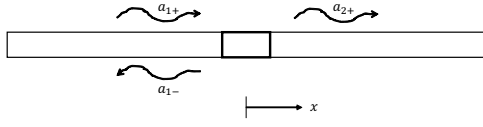


Fig. 7. Two rods coupled through a finite rod joint

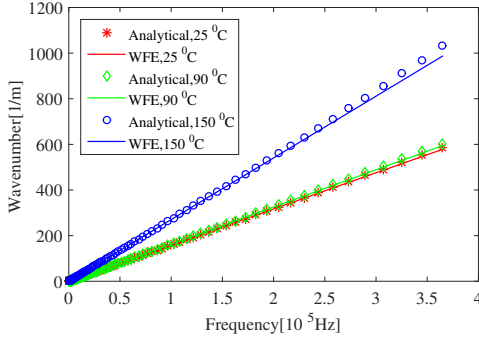


Fig. 8. Predicted temperature dependent dispersion curves for the rod

A. Two Collinear rods coupled through a finite rod

Consider two similar and collinear long rods undergoing longitudinal vibration. A finite rod of a different material properties is sandwiched between them as shown in Fig. (7). Cross-sectional areas $A_1 = A_2 = A_J = 0.003m^2$, lengths $L_1 = L_2 = 0.2m$ and $L = 0.003m$. Both rods are made of carbon epoxy while the coupling joint is made of honeycomb foam (Table I).

The results of the analytically [26] and numerically obtained wave dispersion relation and interaction coefficients for the problem are presented in Figs. (8) and (9)

Excellent agreement is observed between the analytically and numerically obtained results with little deviation at high frequency due to FE discritisation errors. The results also show a linear proportional increase in the interaction coefficient with respect to temperature. The proportional increment is observed until the glass transition temperature ($110^\circ C$), beyond this temperature, the coefficient value decreases proportionally.

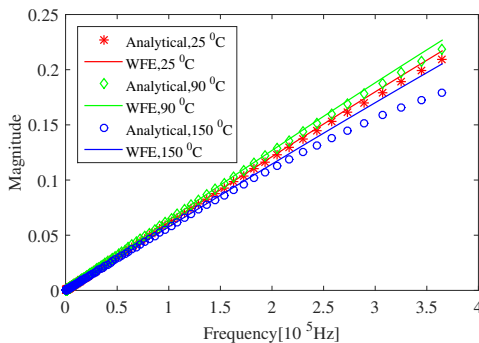
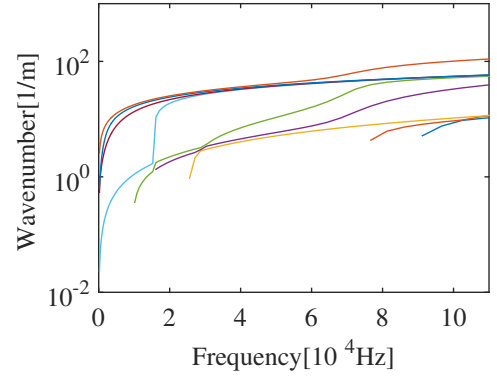
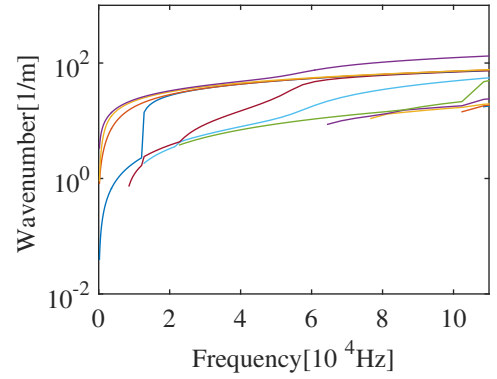


Fig. 9. Predicted temperature dependent reflection coefficients for a finite joint connecting two rods



(a) $25^\circ C$



(b) $150^\circ C$

Fig. 10. Dispersion relations for waves in the composite laminate at $25^\circ C$ and $150^\circ C$

B. Composite laminate

Two collinear composite laminates connected by through a coupling joint (another composite panel on which damage is modelled) of the same cross-section ($5mm \times 10mm$). A periodic segment of the quasi-isotropic sandwich panel comprises of a honeycomb foam core sandwiched between two carbon fibre facesheets. The temperature dependent mechanical properties (elastic and shear moduli) and their respective material loss factor of the materials are presented in Figs. 3 and 4. The thickness of the core, h_c , is 10 mm while that of the facesheet, h_f , is 1 mm. The length of the coupling joint is 3mm while that of each waveguide is arbitrary, as only a periodic segment (as shown in Fig. 6) is needed for the WFE model.

Surface breaking crack of 1mm width and 2mm depth located at 1mm along the length of the coupling joint. The crack is modelled through the node duplication approach [27].

Temperature dependent dispersion curves for the propagating waves within the system are shown in Figs. 10 and 11.

Four propagating waves, in-plane and out-of-plane flexural waves as well as torsional and axial waves, exist below the frequency of 10 kHz. The cut-on frequencies and number of waves within the considered frequency range depend on temperature as shown in Fig. 10.

While at $25^\circ C$, there are nine waves within the the frequency range with cut-ons occurring at about 10kHz, 18kHz,

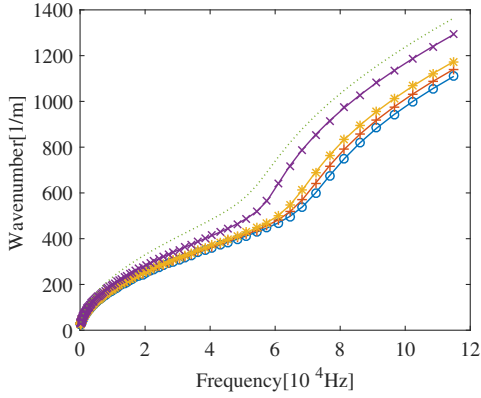


Fig. 11. Dispersion relations for torsional waves in the composite laminate at -100°C (o), 25°C (+), 90°C (*), 110°C (x) and 150°C (···)

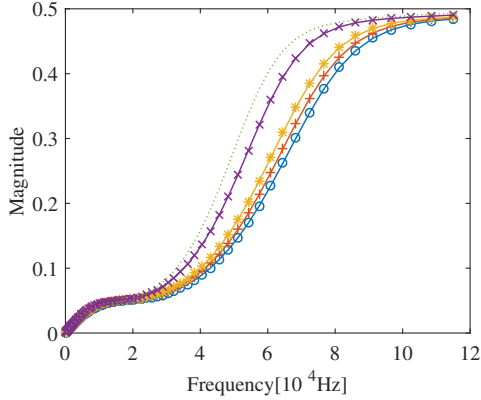


Fig. 12. The temperature dependent reflection coefficient magnitude of the flexural wave from cracked joint of the composite laminate at -100°C (o), 25°C (+), 90°C (*), 110°C (x) and 150°C (···)

25kHz, 75kHz and 90kHz as shown in Fig. 10a, there are eleven waves at 150°C , with cut-ons occurring at about 10kHz, 12kHz, 22kHz, 68kHz, 78kHz, 102kHz and 109kHz as shown in Fig. 10b. The effect of temperature on the wavenumber magnitude can be analysed using the temperature dependent torsional wave dispersion relation shown in Fig. 11. There is a difference of about 30% between the wavenumbers at -100°C , 25°C and 90°C , and at 150°C . The variation in the waves properties as a function of temperature can be said to be as a result of the variation in the material properties and material loss factor at different temperature.

Results of the reflection coefficients magnitude of the propagating waves are presented in Figs. (12), (13) and (14).

Scattering coefficient trends of the axial and torsional waves show more sensitivity to change in temperature at higher frequencies in the range above 60kHz, while that of the flexural wave shows significant difference only in the range 25kHz to 85kHz but insignificant to temperature change outside this frequency range. The overall difference of the scattering coefficients in these two temperature ranges (before and after glass transition) for all the waves is about 50%. However, the effect of temperature on the reflection coefficient

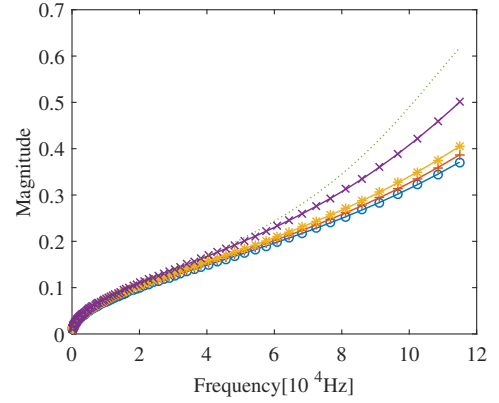


Fig. 13. The temperature dependent reflection coefficient magnitude of the torsional wave from cracked joint of the composite laminate at -100°C (o), 25°C (+), 90°C (*), 110°C (x) and 150°C (···)

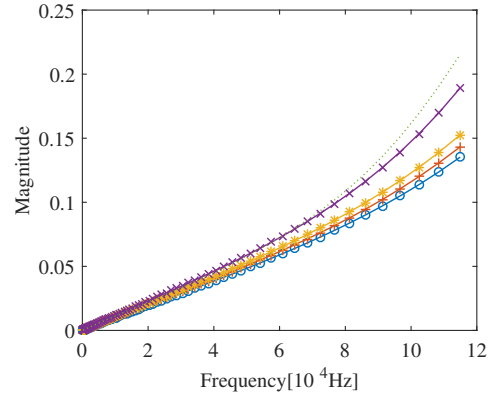


Fig. 14. The temperature dependent reflection coefficient magnitude of the axial wave from cracked joint of the composite laminate at -100°C (o), 25°C (+), 90°C (*), 110°C (x) and 150°C (···)

below, within and after the glass transition temperature varies significantly. Below the glass transition temperature, there exist slight increase in the reflection coefficients of all the wave types with a maximum difference of about 10% per 50°C change in temperature. Above the glass transition temperature, a considerable difference is observed with respect to temperature change with an observed difference of about 28% per 50°C change in temperature.

VI. CONCLUDING REMARKS

The temperature dependent mechanical characteristics of a quasi-isotropic sandwich laminate are presented in this article. The composite is made of two materials, carbon epoxy facesheet, impregnated in the resin and draped over the mould, and a quasi-isotropic honeycomb core. The thermomechanical characteristics of each of these materials are separately measured experimentally and it is observed that there is a large divergence of the material loss factor, elastic and shear moduli especially within and above the glass transition temperature of the resin. The thermomechanical characteristics are then used to determine the temperature dependent wave propagation properties of the panel using a wave finite element approach.

The panel is then idealised as a system of two waveguide segments connected through a coupling joint. The wave finite element modelling of each waveguide segment is then coupled with the full finite element of the coupling joint, on which damage is modelled, in order to calculate the scattering coefficients of the waves interaction with the damage. As in the case of the experimental results for the moduli and the material loss factor, the numerical predicted wave propagation properties and the wave scattering coefficients exhibit notable differences in their results before the glass transition temperature compared to after the glass transition temperature. It can be concluded that temperature is a significant factor that should be taken into consideration in the design process of aerospace material in order to improve its wave response performance.

REFERENCES

- [1] A. Noor and U. Burton, "Computational models for high temperature multilayered composite plates and shells," *Appl Mech Rev*, vol. 45, no. 10, pp. 419–446, 1992.
- [2] Y. Dimitrienko, "Thermomechanical behaviour of composite materials and structures under high temperature: 1. materials, composites," *Part A. Applied Science and Manufacturing*, vol. 28, pp. 463–471, 1997.
- [3] —, "Thermomechanical behaviour of composite materials and structures under high temperature: 2. structures, composites," *Part A. Applied Science and Manufacturing*, vol. 28, pp. 453–461, 1997.
- [4] G. McNally, M. McCourt, and P. Spedding, "The effect of rapid high temperature excursions on the moisture absorption and dynamic mechanical properties of carbon fibre epoxy composite materials, development in chemical engineering and mineral processing," *Asia-Pacific Journal of Chemical Engineering*, vol. 12, no. 1, pp. 169–178, 2004.
- [5] O. Putkis, D. R. P., and C. A. J., "The influence of temperature variations on ultrasonic guided waves in anisotropic cfrp plates," *Ultrasonic*, vol. 60, pp. 109–116, 2015.
- [6] W. J. Zhou and M. N. Ichchou, "Wave scattering by local defect in structural waveguide through wave finite element method," *Structural Health Monitoring*, vol. 10, no. 4, pp. 335–349, 2011.
- [7] J. Renno and B. Mace, "Calculation of reflection and transmission coefficients of joints using a hybrid element/wave and finite element approach," *Journal of Sound and Vibration*, vol. 332, pp. 2149–2164, 2013.
- [8] —, "Vibration modelling of structural networks using a hybrid finite element/wave and finite element approach," *Wave Motion*, vol. 51, no. 4, pp. 566–580, 2014.
- [9] E. Manconi and B. Mace, "Modelling wave propagation in two-dimensional structures using finite element analysis," *ISVR Technical Memorandum*, vol. 318, no. 4–5, pp. 884–902, 2008.
- [10] D. Chronopoulos, B. Troclet, M. Ichchou, and J. Laine, "A unified approach for the broadband vibroacoustic response of composite shells," *Composites Part B: Engineering*, vol. 43, no. 4, pp. 1837–1846, 2012.
- [11] D. Chronopoulos, B. Troclet, O. Bareille, and M. Ichchou, "Modeling the response of composite panels by a dynamic stiffness approach," *Composite Structures*, vol. 96, pp. 111–120, 2013.
- [12] D. Chronopoulos, M. Ichchou, B. Troclet, and O. Bareille, "Efficient prediction of the response of layered shells by a dynamic stiffness approach," *Composite Structures*, vol. 97, pp. 401–404, 2013.
- [13] —, "Predicting the broadband vibroacoustic response of systems subject to aeroacoustic loads by a krylov subspace reduction," *Applied Acoustics*, vol. 74, no. 12, pp. 1394–1405, 2013.
- [14] —, "Thermal effects on the sound transmission through aerospace composite structures," *Aerospace Science and Technology*, vol. 30, no. 1, pp. 192–199, 2013.
- [15] —, "Predicting the broadband response of a layered cone-cylinder-cone shell," *Composite Structures*, vol. 107, no. 1, pp. 149–159, 2014.
- [16] —, "Computing the broadband vibroacoustic response of arbitrarily thick layered panels by a wave finite element approach," *Applied Acoustics*, vol. 77, pp. 89–98, 2014.
- [17] V. Polenta, S. Garvey, D. Chronopoulos, A. Long, and H. Morvan, "Optimal internal pressurisation of cylindrical shells for maximising their critical bending load," *Thin-Walled Structures*, vol. 87, pp. 133–138, 2015.
- [18] T. Ampatzidis and D. Chronopoulos, "Acoustic transmission properties of pressurised and pre-stressed composite structures," *Composite Structures*, vol. 152, pp. 900–912, 2016.
- [19] I. Antoniadis, D. Chronopoulos, V. Spitas, and D. Koulocheris, "Hyper-damping properties of a stiff and stable linear oscillator with a negative stiffness element," *Journal of Sound and Vibration*, vol. 346, no. 1, pp. 37–52, 2015.
- [20] D. Chronopoulos, M. Collet, and M. Ichchou, "Damping enhancement of composite panels by inclusion of shunted piezoelectric patches: A wave-based modelling approach," *Materials*, vol. 8, no. 2, pp. 815–828, 2015.
- [21] D. Chronopoulos, I. Antoniadis, M. Collet, and M. Ichchou, "Enhancement of wave damping within metamaterials having embedded negative stiffness inclusions," *Wave Motion*, vol. 58, pp. 165–179, 2015.
- [22] D. Chronopoulos, "Design optimization of composite structures operating in acoustic environments," *Journal of Sound and Vibration*, vol. 355, pp. 322–344, 2015.
- [23] M. Ben Souf, D. Chronopoulos, M. Ichchou, O. Bareille, and M. Haddar, "On the variability of the sound transmission loss of composite panels through a parametric probabilistic approach," *Journal of Computational Acoustics*, vol. 24, no. 1, 2016.
- [24] D. Chronopoulos, "Wave steering effects in anisotropic composite structures: Direct calculation of the energy skew angle through a finite element scheme," *Ultrasonics*, vol. 73, pp. 43–48, 2017.
- [25] B. R. Mace, D. Duhamel, M. J. Brennan, and L. Hinke, "Finite element prediction of wave motion in structural waveguides," *The Journal of the Acoustical Society of America*, vol. 117, no. 5, pp. 2835–2843, 2005.
- [26] J. Doyle, *Wave Propagation in Structures: Spectral Analysis Using Fast Discrete Fourier Transforms*. Springer, 1997.
- [27] M. Lowe, C. P., J. Kao, and O. Diligent, "The low frequency reflection characteristics of the fundamental antisymmetric lamb wave a_0 from a rectangular notch in a plate," *The Journal of the Acoustical Society of America*, vol. 112, no. 6, pp. 2612–2622, 2002.